A Numerical Parametric Study of SAR from a Dual-Band PIFA Based Antenna for Mobile Communication

Serdar Okuyucu[1], Mustafa Seçmen[1], Korkut Yeğin[2], Başak Özbakış[3]

[1]Department of Electrical and Electronics Engineering, Yaşar University, İzmir, Turkey
serdar.okuyucu@yasar.edu.tr, mustafa.secmen@yasar.edu.tr
[2]Department of Electrical and Electronics Engineering, Ege University, İzmir, Turkey
korkut.yegin@ege.edu.tr
[3]R&D Department, Vestel Inc., Manisa, Turkey
basak.ozbakis@vestel.com.tr

Abstract

Specific Absorption Rate (SAR) analysis is a vital part of compliance tests for commercial mobile phones performed in accordance with the set of comprehensive standardized practices provided by authoritative bodies. Dependence of SAR on a variety of parameters, with the structure of the handset pronounced the most, calls for bringing in the SAR analysis of various types of phones into the field of study for reference. This paper focuses on the SAR analysis of a PIFA based mobile phone antenna when operated next to standardized and anatomically correct head models. The effect of averaging method used, positioning of the phone, frequency of operation, and the presence of a homogeneous hand model on SAR is investigated along with the antenna performance in terms of terminal and radiational characteristics.

1. Introduction

The progress shown in mobile phone technology in providing multiple band transmission with high data rates has enabled the incorporation of new functionalities and rich content mobile services in modern smart mobile phone terminals. The cellular device antennas receive and radiate electromagnetic energy at different frequencies depending on the type of application in use. At these frequencies, human body tissues are characterized as lossy dielectric materials. Since cell phones are used in close proximity of the head, high energy electromagnetic waves are able to penetrate through and be absorbed by the tissue which may result in serious health hazards by causing a temperature increase in various parts of the brain.

As a dosimetric measure of the rate at which the energy is absorbed by the body exposed to radio frequency electric fields, Specific Absorption Rate (SAR) is defined as the time derivative of incremental energy absorbed by an incremental mass contained in a volume element of a given density [1], given as,

$$SAR = \frac{d}{dt}\left(\frac{dW}{dm}\right) = \frac{d}{dt}\left(\frac{dW}{\rho dV}\right) \quad (1)$$

In terms of the induced electric field, it is given as,

$$SAR = \frac{\sigma E^2}{2\rho} \quad (2)$$

In (2), E is the peak electrical field strength in the body tissue (V/m), σ is the tissue conductivity (S/m), and ρ is the mass density of the tissue (kg/m^3). SAR is usually quoted as a peak spatial average value averaged over the whole body or a small sample volume of tissue containing a certain amount of mass ($1g$ or $10g$) and it is given in units of W/kg. In order to ensure a safe operation, the compliance testing and certification of mobile terminals in each country are subject to measurement protocols of peak spatial average SAR specified by authoritative bodies (i.e. IEEE, FCC, ICNIRP).

The SAR distribution in the human body due to exposure to electromagnetic fields is effected by several factors such as, anatomy of the head, phone position, frequency, tissue composition, EM source structure, and electrical properties of tissues. In [2] and [3], significant SAR changes with nonlinear dependence characteristics were observed due to the effect of inclination angle between antenna and head model. Muscle and tissue distribution inside anatomical models is one major factor influencing spatial peak SAR [4]. In [5], a significant increase of 2.2-4.7 dB of peak spatial SAR was found when tissue distribution of exposed regions was considered instead of standard liquids in different parts of the body.

Regarding the inclusion of a hand model in SAR analysis, research shows that it may result in a decrease [6] as well as an increase [7, 8] for specific types of hand grip.

Regarding the morphological properties of the head model, in [9], SAR distribution in the brain was shown to vary between two biological head models due to differences in anatomical proportions and geometry of the head models. In [10], as a result of the comparison of SAR obtained from an adult head model and a child head model, maximum 10 g averaged SAR values were obtained with bigger head model since it provides a large radius of curvature that is similar to a flat phantom where the tissue boundary is closer to the source, thereby absorbing more energy than a smaller head. In [11], the impact of head morphology on local brain SAR was investigated where head morphology was found as an important source of uncertainty for dosimetric studies of mobile phones.

Due to the dependence of SAR on the model of human head used, tissue parameters of the head model and positioning of the phone relative to the head, causes discrepancies in test results obtained from different laboratories for the same wireless handset. In order to overcome inter-laboratory measurement variations, a specific anthropomorphic mannequin (SAM) head model with a standardized size, shape and tissue equivalent liquid parameters have been defined by the IEEE Standards Coordinating Committee 34, Subcommittee 2, Working Group 1

(SCC34/SC2/WG1) [12]. In general terms, the SAM phantom is defined as a low permittivity, low loss plastic shell filled with homogeneous tissue-equivalent liquid. The properties of the homogeneous filler liquid is selected such that it will yield permittivity and conductivity values within $\pm10\%$ of the target values at the frequency of measurement. The phantom shell on the other hand should be constructed from low-permittivity, low-loss material with loss tangent less than or equal to 0.05 and a relative permittivity between 2 and 5. As an accurate and practical representation of the pinna, the phantom shell also includes a simplified lossless spacer with a thickness of 6mm.

For the evaluation of repeatability in SAR using standardized techniques, an international inter-laboratory comparison was made between 10 laboratories where three different commercially available mobile phone models were used as the radiation source [13]. As a result, agreement in calculated SAR between the participating laboratories was found to be similar to the agreement obtained in inter-laboratory comparisons. Regarding the conservativeness of SAM phantom, in [14], SAM phantom was compared with four anatomical head models at different ages for exposure from a typical bar-type phone. As a result, SAM phantom was found conservative for phone models with the antenna at the top of the phone. However, for phones having antenna at its bottom, SAM phantom was shown to produce lower 1- and 10-g SAR due to the occurrence of hotspot farther from the feed point of the antenna.

As a review of literature on the subject matter shows, it is not always possible to establish a direct relationship between SAR and effecting parameters as to describe how the peak spatial SAR will change with respect to that particular parameter. The measured and numerically calculated values of SAR are highly dependent on type of mobile phone and antenna type under investigation and distribution of SAR from generic source models cannot be extrapolated to real device exposures [15, 16]. For that reason, as a valuable contribution to this field of study, it is important to add to the existing knowledge, the SAR characteristics of various mobile phones analyzed in a way as described in standardized practice. In that sense, it is the purpose of this study to analyze the SAR characteristics produced by the main antenna of a mobile phone where the metallic bottom casing of the handset is configured as a Planar Inverted F Antenna. By numerical simulations, the comparison of SAR distributions caused by the handset in SAM phantom and heterogeneous anatomical head models are made together with an analysis of the effect of using a homogeneous hand model next to the SAM phantom. Effect of positioning the antenna element on bottom and upper parts of the handset and SAR averaging methods are considered.

2. Models and Methods of Numerical Simulations

2.1 Phone Model

As the source of electromagnetic radiation, a dual band (GSM 900 MHz and 1800 MHz) PIFA antenna element is implemented. The geometry of the phone is shown in Fig. 1 where the height, width, and thickness of the antenna element are 52.9 mm, 5.3 mm, and 0.9 mm respectively.

In this configuration, the printed circuit board (PCB) of the phone is modeled with a FR-4 substrate sandwiched between two thin metal sheets which are connected to each other by interconnecting vias. The PCB is in turn connected at a number of points to the system ground plane located at the screen side of the phone. To model the screen, a glass Pyrex sheet of dimensions 128 mm x 70 mm x 1.3 mm is used in the front side

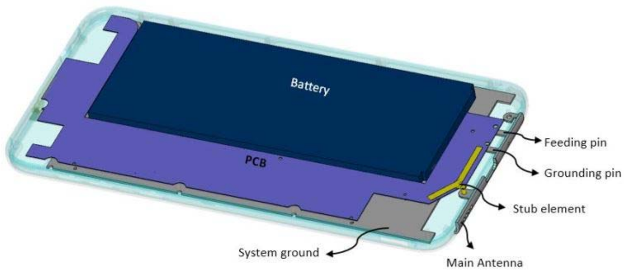

Fig. 1. Geometry of antenna element

of mobile phone. The antenna element is fed through a feeding pin placed at the lower end of the PCB. In order to utilize the bandwidth of the antenna at desired frequencies of interest, namely, 900 MHz and 1800 MHz, the resonance frequency of the antenna is adjusted by use of reactive loading to the grounding pin of the antenna. The simulated return loss $|S_{11}|$ (dB) of the antenna is shown in Figure 2.

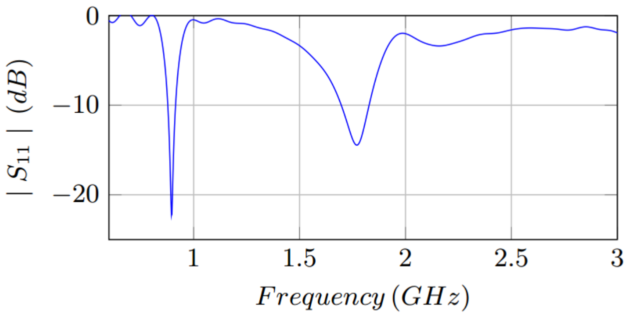

Fig. 2. Return Loss of the antenna shown in Fig. 1.

2.2 Head and Hand Models

For the investigation of the effect of using different head models and inclusion of a hand model on peak spatial average SAR, two different head models and a homogeneous hand model are used in numerical simulations as shown in Fig. 3.

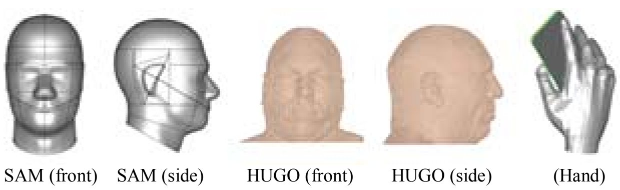

Fig. 3. Head and hand models

2.2.1 SAM Head and Homogeneous Hand Model

The inner and outer surfaces belonging to the left and right halves of the SAM phantom are publicly available as a computer-aided design (CAD) file. In order to use this available model in numerical simulations, the volume enclosed by the inner surface and the volume between the inner surface and the outer shell are solidified by use of a CAD program. The resulting files are imported to the electromagnetic simulation program and the solidified regions are given material properties in accordance with the standards as given in Table 1.

Additionally, a homogeneous hand model, having the same material properties as the SAM liquid, is constructed and the effect of the hand model when placed near the homogeneous SAM head model in two holding positions is investigated.

Table 1. Material properties of SAM and hand at 900 MHz

	ε_r	σ (S/m)	ρ (kg/m3)
SAM liquid	41.5	0.97	1000
SAM shell	3.7	0	1000
Hand	41.5	0.97	1000

2.2.2 Heterogeneous Anatomical Head Model

In order to construct a base of comparison to the SAR obtained from SAM phantom, an anatomically correct head model with 1mm resolution is used in this study. This voxel-based human model is the "HUGO" from the Visible Human Project. The voxel model used is a complete body representation of the human body in an upright standing position and requires the use of additional software [17] to put the body into practical (i.e. phone holding) positions. In this study, the HUGO head model placed next to the phone in two talking positions without the hand is considered.

2.2.2 Test Positions

As a way of simulating the real case talking positions of the phone, two standardized positions ("cheek" and "tilt") of holding the phone against the head phantom are considered.

In placing the phone in the cheek position, two lines are defined on the handset, namely, the vertical centerline and the horizontal line as shown in Fig. 4. The vertical centerline passes through the midpoints of the phone's width at the level of

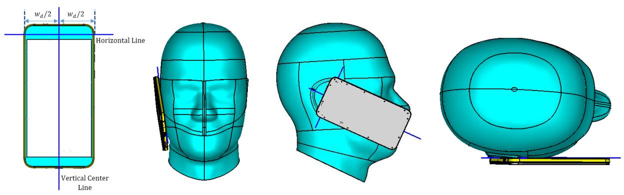

(a) Reference positioning lines and cheek positioning

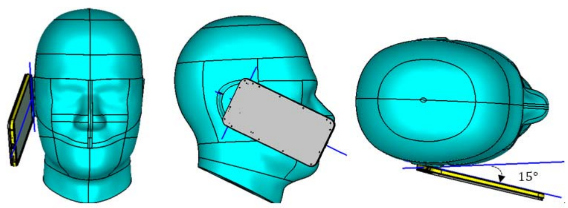

(b) Tilt positioning

Fig. 4. (a) Reference positioning lines and (b) Tilt positioning

acoustic output and bottom edge. The horizontal line passes through the acoustic output in a direction perpendicular to the vertical centerline. The phone is placed next to the phantom such that the intersection of two perpendicular lines is on the extension of the line passing through right ear center (REC) point and left ear center (REC) point. By translation along and rotation around REC-LEC axis, the phone is placed as shown in Fig. 4(a) such that it is in contact with the pinna and a point below the pinna on the cheek.

In positioning the phone in the tilt position, the phone in the cheek position is moved away from the handset and is rotated around the horizontal line by 15 degrees as shown in Fig. 4(b). The handset is then moved towards the phantom on the REC-LEC line until any point of the handset in touch with the ear.

2.2 Simulation Settings

The simulations of the described model setup were performed on a hexahedral mesh using the transient solver of microwave studio of computer simulation technology (CST). For the excitation of the antenna, a discrete port with an impedance of 50 ohms was defined at the feed point of the antenna. The frequency range is set between 600 MHz and 3 GHz and far field, electric field, and power loss monitors were set at 900 MHz and 1800 MHz. In the post-processing phase of the simulation, the 1 g and 10 g spatial peak volume averaged SAR calculations of all configurations were performed at the two frequencies of interest. In each configuration, the averaged SAR values are normalized with respect to the power accepted by the antenna. The reference average output power is set to 0.25 W and 0.125 W at the respective frequencies of 900 MHz and 1800 MHz respectively, which represents the 1/8 of the peak output power of an actual handset. The normalization with respect to the average power compensates for the occurrence of antenna mismatches when using the phone in close proximity of different head and hand model configurations.

3. Results and Discussion

In the analysis of SAR characteristics observed due to electromagnetic radiation from the described handset, the constructed models of homogeneous head (SAM), heterogeneous anatomical head, and homogeneous hand models are used in a number of various configurations. The numerical SAR calculation of these configurations are carried out by considering cheek and tilt positions, 1g and 10g spatial average, antenna position in upper and bottom side of the phone, and frequency of operation. Analyzing the resulting spatial average SAR data given in Table 2 where each row represents a single type of configuration analyzed at different frequencies and averaging schemes, it is immediately obvious that for every configuration, the SAR value is lower at higher 1800 MHz when compared with that obtained at 900 MHz for both methods of averaging used. This lower SAR characteristic at higher frequency can be related to lower power output (0.125W) defined at 1800 MHz when compared to that (0.25 W) defined at 900 MHz. The averaging method used also has a slight effect on peak spatial average SAR where averaging over a 10g of tissue results in lower peak values when compared with 1g averaging. This is due to the averaging at points of high power absorption together with neighbor areas with lower power absorptions. The use of 10g averaging causes the spatial smoothing of SAR distribution, making it harder for the detection of closely spaced points of peak SAR. Except for the HUGO model with antenna placed at upper part of the phone, the tilting position of the phone is seen to reduce SAR to some degree when compared with cheek positioning. This is mostly due to the decrease in coupling between the head tissue and antenna element together with the system ground plane, which is caused by the decrease in parallel positioning between the two by tilting. The effect of tilting is better recognized at 900 MHz since at relatively low frequencies, the chassis mode currents are more pronounced than the antenna element itself for PIFA antennas. For all configurations of SAM and HUGO head where the inclusion of hand is not considered, the placement of the antenna at the upper part is seen to produce higher SAR near the

Table 2. SAR distribution for each configuration

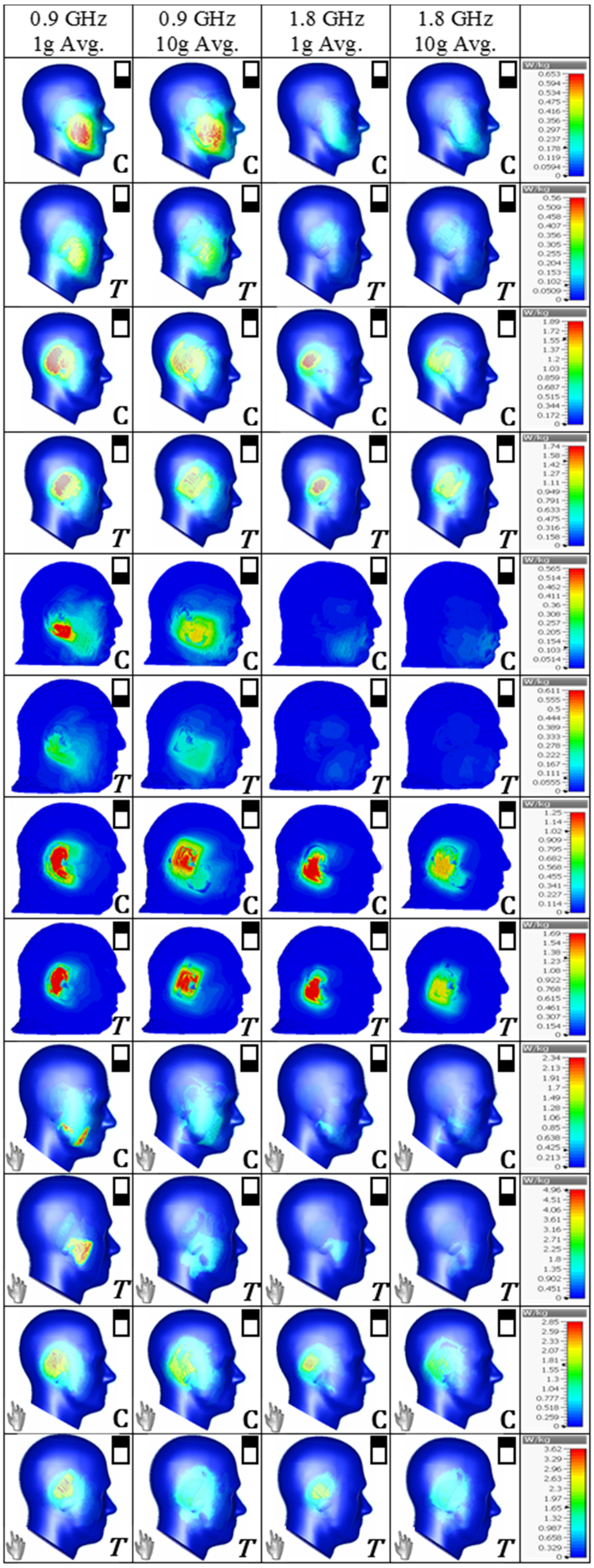

: Phone down : Phone up **C**: Cheek *T*: Tilt : With hand

pinna due to the decreased distance between antenna and head tissue.

The various use configurations considered in this paper affect not only the SAR values but the performance of antenna element by a significant amount.

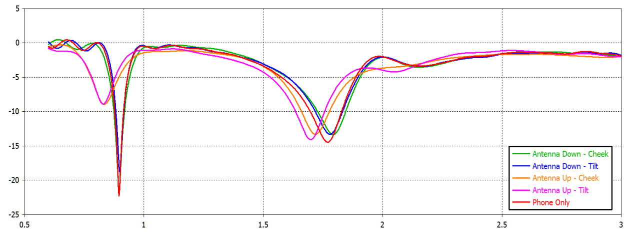

Fig. 5. $|S_{11}|(dB)$ for SAM phantom used in four configurations

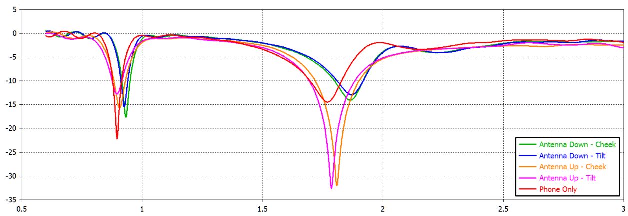

Fig. 6. $|S_{11}|(dB)$ for HUGO head used in four configurations

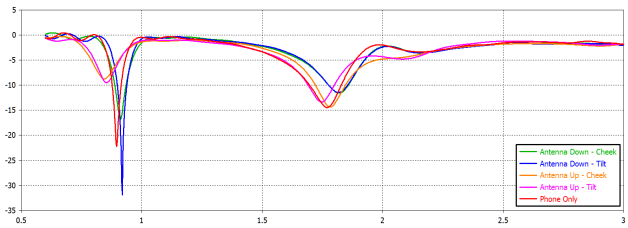

Fig. 7. $|S_{11}|(dB)$ for SAM phantom used with homogeneous hand in four configurations

With reference to Figures 5 and 7, even though the cheek and tilt positioning does not have a significant effect, the placement of the antenna at the upper side of the phone by rotating the handset by 180 around its center axis, decreases frequency of resonance due to the reactive loading to the antenna by the head placed in the antenna's near field. For the case of HUGO model shown in Fig. 6, the trend of decreased frequency of resonance occurs for the case where antenna is placed at the upper side of the phone. For other configurations, resonance characteristics is seen to stay relatively invariant.

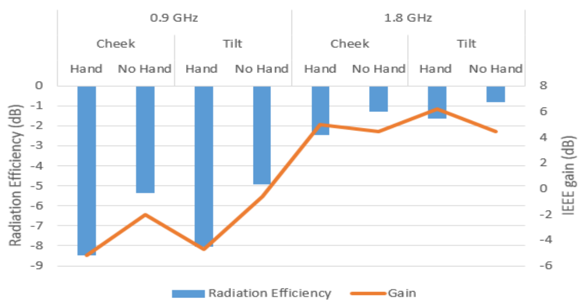

Fig. 8. Gain and radiation efficiency of antenna in use positions

In Figure 8, the gain and radiation characteristics of the configurations utilizing SAM phantom are shown. The inclusion of the hand model is seen to reduce the radiation efficiency for all configurations. For the gain, the trend is towards a decrease with the inclusion of hand at 900 MHz. Nevertheless, it shows a slight increase at 1800 MHz. Under the same set of configurations, higher gains by up to 6 dB are noted at 1800 MHz when compared with the gain at 900 MHz.

6. Conclusions

In this study, the SAR analysis of a dual band PIFA based main antenna element of a mobile phone terminal has been performed by numerical simulations. The change in spatial average SAR with respect to head type, talk positions, antenna location, averaging method used and the presence of a homogeneous hand has been investigated. In overall, relatively low peak spatial SAR values were obtained at higher frequency of operation due to a reduced peak output power available from the antenna at this frequency. The 10g averaging method was found to provide lower SAR values when compared to that obtained from 1g averaging. The positioning of the antenna element was found as the most influential parameter on SAR which produced SAR values even higher than standardized maximum limits when placed near the pinna, at the upper part of the phone. For that reason, the use of antenna on upper part of the was found as impractical and was not considered in the analysis of the effect of a hand on SAR and terminal characteristics of the antenna. The presence of a homogeneous hand holding the mobile handset was noted to degrade the radiation efficiency of the antenna and had an increasing effect on SAR when compared with the cases utilizing no hand model. In some configurations, the peak spatial average SAR values obtained from heterogeneous anatomical head models were higher around the pinna than its standard SAM head counterpart. This difference in SAR is a result of the difference in terms of how the pinna is modeled in two models. Since a lossless spacer is used as a model of pinna in SAM model, this model produced lower SAR values in the pinna when compared with HUGO head model. Use of homogeneous head and hand models next to the mobile handset resulted in a down-shift in the frequency of resonance of the antenna. Due to the complex structure of the heterogeneous head model, this characteristic was shown to be dependent on use positions and positioning of the antenna.

7. Acknowledgements

This work is partly funded by The Scientific and Research Council of Turkey (TUBITAK) under grant numbers: 1005.STZ.2015, TEYDEB 3151039, and Vestel Electronics Inc.

8. References

[1] IEEE Recommended Practice for Determining the Peak Spatial-Average Specific Absorption Rate (SAR) in the Human Head from Wireless Communications Devices: Measurement Techniques, IEEE Std 1528-2013

[2] Hossain, M.I., M.R.I. Faruque, and M.T. Islam. "Original research: Analysis on the effect of the distances and inclination angles between human head and mobile phone on SAR." Progress in Biophysics And Molecular Biology 119, (November 1, 2015): 103-110.

[3] Satriya, A.B. Setijadi, E. "An Analysis Method of Effect of Linear Polarized Electromagnetic Exposure from Mobile Phone to Human Head with Various Incident Angles", Int. Conf. on Information Tech. and Electrical Engineering (ICITEE) 2013 International Conference, pp. 266-270

[4] Lee, AK, and J Yun. n.d. "A Comparison of Specific Absorption Rates in SAM Phantom and Child Head Models at 835 and 1900 MHz." IEEE Transactions On Electromagnetic Compatibility 53, no. 3: 619-627.

[5] Christ, Andreas, Klingenbock, Anja, Samaras Theodoros, Goiceanu Cristian, Kuster Niels." The Dependence of Electromagnetic Far-Field Absorption on Body Tissue Composition in the Frequency Range from 300 MHz to 6 GHz" IEEE Transactions on Microwave Theory & Techniques, May 2006, Vol. 54 Issue 5, p2188-2195.

[6] Hossain, Md. Ikbal, M.R. Iqbal Faruque, and M. Tariqul Islam. 2015. "Original: Investigation of hand impact on PIFA performances and SAR in human head." Journal Of Applied Research And Technology 13, 447-453.

[7] Li, CH, M Douglas, E Ofli, B Derat, S Gabriel, N Chavannes, and N Kuster. n.d. "Influence of the Hand on the Specific Absorption Rate in the Head." IEEE Trans. on Antennas and Propagation 60, no. 2: 1066-1074.

[8] Panagamuwa, C.J., Howells, I. Kotb, A. "Use of a block hand phantom for mobile phone Specific Absorption Rate measurements." 2013, 7Th European Conference on Antennas and Propagation (Eucap)

[9] Ghanmi, Amal, Nadège Varsier, Abdelhamid Hadjem, Emmanuelle Conil, Odile Picon, and Joe Wiart. 2013. "Electromagnetic fields: from dosimetry to human health: Study of the influence of the laterality of mobile phone use on the SAR induced in two head models." Comptes Rendus - Physique 14, 418-424.

[10] Monebhurrun, V, "Conservativeness of the SAM Phantom for the SAR Evaluation in the Child's Head." IEEE Transactions On, IEEE Trans. Magn no. 8: 3477

[11] Adibzadeh, F., J.F. Bakker, M.M. Paulides, R.F. Verhaart, and G.C. van Rhoon. 2015. "Impact of head morphology on local brain specific absorption rate from exposure to mobile phone radiation." Bioelectromagnetics 36, no. 1: 66-76.

[12] Beard, B.B., et.al., "Comparisons of computed mobile phone induced SAR in the SAM phantom to that in anatomically correct models of the human head", IEEE Trans. Electromagn. Compat. Electromagnetic Compatibility, IEEE Transactions on. 48(2):397-407

[13] Siegbahn, M., "An International Interlaboratory Comparison of Mobile Phone SAR Calculation with CAD-Based Models", IEEE Trans. Electromagn. Compat., 52(4):804-811 Nov, 2010

[14] Lee, A.-K., et al. "SAR Comparison of SAM Phantom and Anatomical Head Models for a Typical Bar-Type Phone Model." IEEE Trans. on Electromagn. Compat. 57, no. 5 (October 1, 2015): 1281-1284.

[15] Ghanmi, Amal, et. al., "Electromagnetic fields: from dosimetry to human health: Study of the influence of the laterality of mobile phone use on the SAR induced in two head models." Comptes Rendus - Physique 14, 418-424.

[16] Keshvari, Jafar, and Teemu Heikkilä. 2011. "Review: Volume-averaged SAR in adult and child head models when using mobile phones: A computational study with detailed CAD-based models of commercial mobile phones." Progress in Biophysics and Molecular Biology 107, no. Non-Ionizing Radiation (NIR) and Children's Health: 439-442.

[17] M., Vuchkovikj, Munteanu I., and Weiland T. 2013. "Application of postured human model for SAR measurements." Advances in Radio Science, Vol 11, pp 347-352 (2013) 347.